Computational spectral analysis of wave propagation in linear elastodynamics

José Ortiz-Ocampo

April 23, 2024

Abstract

This project investigates the spectral properties of the differential operator associated with wave propagation in two-dimensional linear elastodynamics. Starting from variational principles, we derived the weak form of the governing differential equations and performed a finite element method (FEM) discretization to obtain a finite-dimensional approximation of the operator. This approach enabled the estimation of eigenvalues and eigenfunctions, providing insights into their behavior across different geometric domains.

We focused on two primary aspects of spectral analysis: the isospectrality of domains that present isospectrality with respect to the Laplacian, and the verification of a relation as Weyl's law for this operator. Our findings indicate that domains isospectral under the Laplacian operator do not necessarily retain this property under the studied operator, suggesting the need for further theoretical exploration to determine the necessary geometric conditions for isospectrality. Additionally, while verifying Weyl's law, we observed that the coefficient relating the domain area to eigenvalue growth rate presents a dependence with the domain geometry, underscoring the importance of the domain's shape in spectral analysis.

Future studies should expand on the variety of domain geometries tested and integrate a more theoretical framework to deepen understanding of these phenomena. The results contribute valuable empirical data to support theoretical investigations into the mathematical structures of wave propagation operators in elastodynamics. Further exploration into the impact of material parameter variations could also provide significant insights for subsequent research.

1 Introduction

Wave propagation in linear, continuum media has been widely studied and applied in a variety of practical scenarios [1], [2]. For the same reason, the study of the differential equations that model this phenomenon maintains their importance, as their continuous exploration enables further enhancement of the methods used for the simulation and further understanding of their mathematical behavior.

One of the areas from which further analysis is in place is spectral analysis: the study of the behavior of the eigenvalues and eigenfunctions of the related operator of the differential equation. In this line, the paper "Can you hear the shape of a drum?" [3], posed the question of whether it was possible to calculate the shape of a domain based on the eigenvalues of the Laplacian operator which modeled the system, that is

$$\begin{aligned} \nabla^2 u_n &= \omega_n^2 u_n, u \in \Omega \\ u &= 0, u \in \delta\Omega. \end{aligned} \tag{1}$$

Although later results answer this question negatively, this and many other results obtained around this topic have increased our understanding of the behavior of the solution of differential operators and equations. One of these findings is Weyl's formula, which describes the asymptotic behavior of eigenvalues of the Laplacian operator [4]–[6]. Particularly:

$$\text{vol}(\Omega) = \omega_d^{-1}(2\pi)^{-d} \lim_{R\to\infty} \frac{N(R)}{R^{d/2}}, \tag{2}$$

where d is the dimension of the domain, ω_d is the volume of the unit ball in $\mathbb{R}^d$ is the volume of the domain and $N(R)$ is the number of eigenvalues smaller than R and $\text{vol}(\Omega)$ is the volume of the

domain. Notice this relation also allows the estimation of the area of the domain based on the related eigenvalues.

This project presents similar explorations for the differential operator that governs wave propagation in linear elastodynamics, to enrich our mathematical knowledge around it and in the search of insights in the same direction as the ones previously mentioned for our case.

2 Modeling

A typical approach for the modeling of wave propagation in linear elastodynamics, and mechanics models in general, would start from the dynamic principles applied over a material point, defining degrees of freedom and starting from conservation laws to achieve the corresponding kinematic equations in terms of differential equations. Although this is a common and perfectly correct approach, we prefer to model the system parting from the the dynamic variational principles, which yields the same results as the approach previously mentioned, but with the additional advantage of arriving to the equations in the the weak formulation faster. That is, the use of variational principles yields integral equations that are ready for the discretization and implementation of FEM method

Consider then a continuum body V that follows a classical behavior. Its kinetic energy is described as [7]

$$T = \int_V \frac{1}{2}\rho \dot{u}_i \dot{u}_i \, \mathrm{d}V \,, \tag{3}$$

in index notation and following Einstein sum convention, where ρ is the density of the body and u_i is the ith component of the displacement vector. On the other hand, its inner potential energy is given by

$$V = \int_V \frac{1}{2}\epsilon_{ij} C_{ijkl} \epsilon kj \, \mathrm{d}V \,, \tag{4}$$

where ϵ_{ij} is the i,j component of the deformation tensor and C_{ijkl} is the corresponding component of the stiffness tensor. The body also possesses an external potential energy, that encompasses the energy due to body forces and surface traction (forces applied in the volume or the surface respectively). However, for the calculation of eigenmodes this term is null.

With the previous terms we are able to construct the Lagrangian, calculate the action functional and minimize it to arrive to the time-domain differential equations to solve. However, we are interested in the frequency-domain solutions, as we are calculating the eigenmodes. In that case, we are allowed to propose a frequency-domain action functional directly, and minimize it, arriving to the frequency-domain solution directly. This is called the *Principle of Correlated Action* [8], and the corresponding action, without external potential energy is given by

$$\mathcal{A}[u;\omega] = \frac{1}{2}\int_V e^*_{ij} C_{ijkl} e_{kl} \, \mathrm{d}V - \frac{\omega^2}{2}\int_V u^*_i \rho u_i \, \mathrm{d}V \,. \tag{5}$$

In the previous equation, the * sign denotes complex conjugate, due to the complex nature of quantities in the frequency domain.

The first variation of this functional is given by

$$\delta\mathcal{A} = \frac{1}{2}\int_V \delta e^*_{ij} C_{ijkl} e_{kl} \, \mathrm{d}V - \frac{\omega^2}{2}\int_V \delta u^*_i \rho u_i \, \mathrm{d}V = 0. \tag{6}$$

Once again, we could apply the variation operator here, and derive the corresponding differential equations. However, to implement the FEM method it is more convenient to discretize at this point, thus turning the functional minimization problem into a typical function minimization one. To discretize the equation, we apply the interpolation operators

$$\begin{aligned} u_i &= N^Q_i u^Q, \\ \epsilon_{ij} &= B^Q_{ij} u^Q, \end{aligned} \tag{7}$$

where N_i^Q denotes the operator required to approximate the i-th displacement component from the values u^Q in the nodes. In the same way, B_{ij}^Q yields the estimated values of the deformation tensor based on the displacement values on the nodes. Refer to [9] to check the explicit forms of this operators in terms of the interpolation functions.

Due to this rewriting, $\delta\epsilon_{ij}^*$ and δu_i^* are applied to u^Q values by means of the chain rule analog to the variation operator. In other words, the resulting equation after discretization is given by

$$\delta\mathcal{A} = \delta u^{Q*}\left[\int_V (B_{ij}^Q)(C_{ijkl})(B_{kl}^P)\,\mathrm{d}V\right]u^P - \rho\omega^2\delta u^{Q*}\left[\int_V ({}_uN_i^Q)({}_uN_i^P)\,\mathrm{d}V\right]u^P = 0. \tag{8}$$

Using the arbitrariness of δu^{Q*}, we finally obtain a matrix system of the form

$$[K^{QP}]\{u^P\} = \omega^2[M^{QP}]\{u^P\}, \tag{9}$$

where $K^{QP} = \int_V (B_{ij}^Q)(C_{ijkl})(B_{kl}^P)\,\mathrm{d}V$ and $M^{QP} = \rho\omega^2\int_V (N_i^Q)(N_i^p)\,\mathrm{d}V$ are the components of the local matrices to calculate via Gaussian integration.

As a final remark, notice that the equation in 9 yields a generalized eigenvalues and eigenfunctions problem [10], where the eigenvalues correspond to the square of the frequencies of the modes, and the eigenfunctions correspond to the 2-dimensional displacement fields associated.

3 Results

In this section, we present the explorations carried around the isospectrality of the surfaces that are isospectral for the Laplacian operator, and analysis around the growth of the eigenvalues and its relation with the area of the corresponding domain.

3.1 Isospectrality of Laplacian-isospectral domains

We take two pairs of Laplacian-isospectral domains, taken from [11]. In Figure 1 we present the first couple.

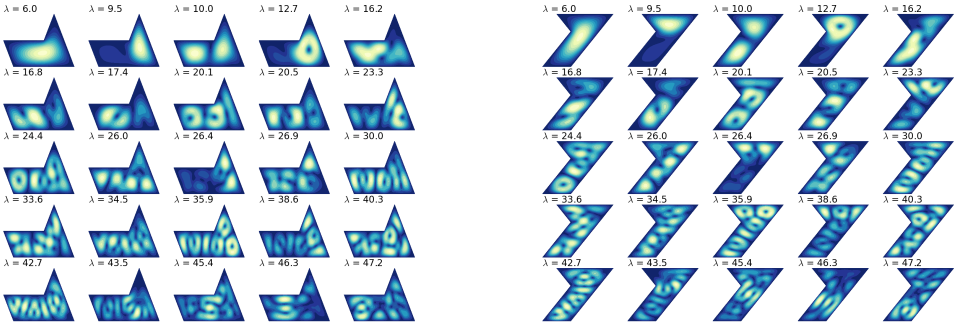

Figure 1: Pair of Laplacian-isospectral domains. Notice they are also isospectral for the wave propagation operator. The norms of the eigenmodes are presented.

From Figure 1, it is noticeable that, at least for the first 25 eigenfunctions, the eigenvalues obtained for both scenarios are approximately the same. Figure 2 presents a deeper comparison for the first 1000 eigenvalues for the domains, as well as their relative (percentage) error.

Notice that, according to Figure 2, the errors stays bounded below 0.5% and present independence with respect their indexes. Furthermore, the eigenvalues curves are overlapped. As this low error can be explained by computational approximation error, these observations helps us conclude that the domains are still isospectral for the operator studied.

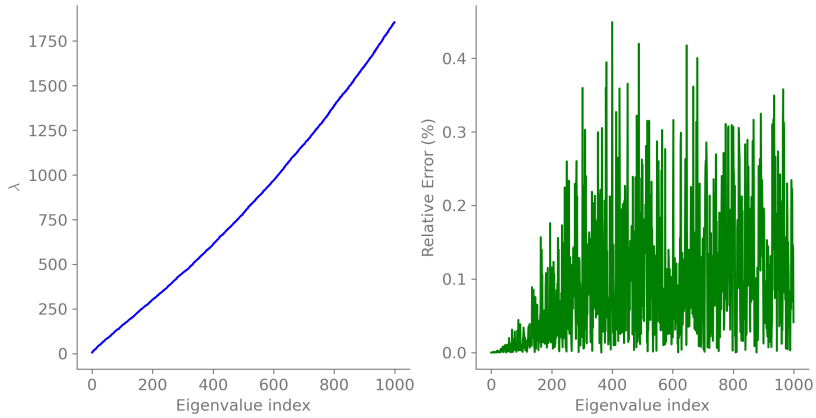

Figure 2: Comparison for the first 1000 eigenvalues for the first pair of domains presented.

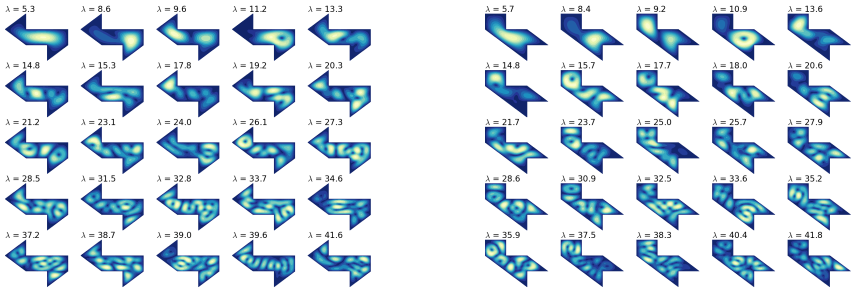

Figure 3: Second pair of Laplacian-isospectral domains tested. In this case, the eigenvalues present a slight difference. The norms of the eigenmodes are presented.

Next, we present the visual and numerical comparisons for the second pair of domains in Figures 3 and 4.

For the second pair of domains we notice errors up to 7%, and typically around 1%, according to Figure 4. Comparing this scenario with the first one presented, the observation point towards a small variation between the eigenvalues of the domains, that is, they do not keep the isospectrality property once studied for the the wave propagation operator.

Overall, we can conclude that not all the domains that are isospectral for the Laplacian operator keep that property for the operator studied. The specific geometric properties that satisfy the domains that kept being isospectral fall outside the scope of this experimental analysis.

3.2 Relation between area and eigenvalues

For 2-dimensional domains, Weyl's law presented in Equation 2 yields

$$A = C \lim_{R\to\infty} \frac{N(R)}{R}, \tag{10}$$

where A is the area and C is a constant, with $C = 4\pi$ for the Laplacian operator. For this exploration, we verify the linear relationship between A and $\lim_{R\to\infty} \frac{N(R)}{R}$. First, we analyze the behavior of $\frac{N(R)}{R}$ when R tends to infinity.

Figure 5 present the behavior of $\frac{N(R)}{R}$ with respect to R. Two geometrical shapes where used in this and following experiments, a square and a isosceles right triangle. The domains where simulated with varying areas, and keeping a 1:10 ratio between the side of the geometries and the characteristic length of the elements in the mesh.

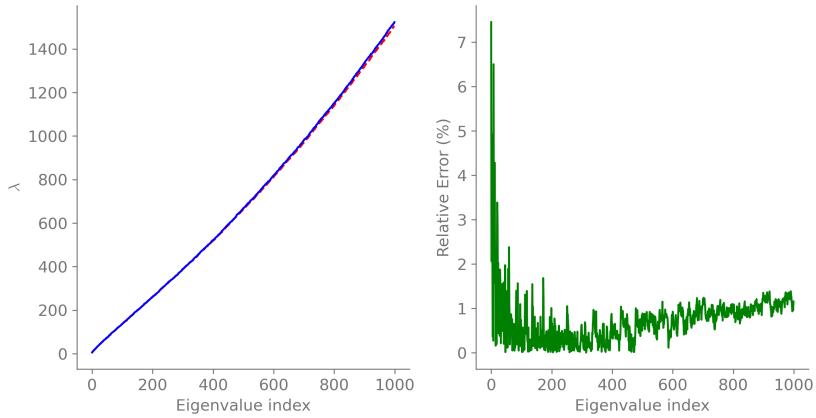

Figure 4: Comparison for the first 1000: eigenvalues for the first pair of domains presented.

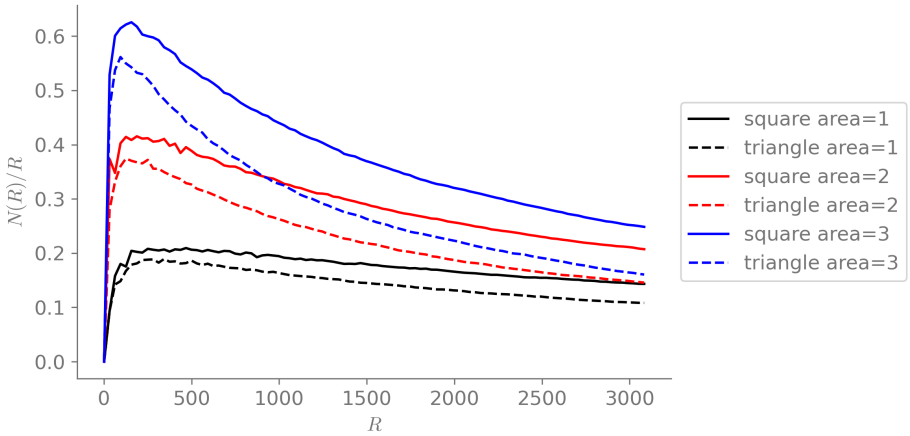

Figure 5: Behavior of $\frac{N(R)}{R}$ as R tends to infinity. Continuous line for squares, dashed for triangles

There are several important observations to be done around Figure 5. First, notice that the values of $\frac{N(R)}{R}$ converge as R increases, which is a first important verification. Second, notice that the convergence values increase as the area increases, which poses a direct proportionality relation between A and $\lim_{R\to\infty} \frac{N(R)}{R}$, which is a second verification towards an analog of Weyl's law for this operator. Finally, we notice that, although plots corresponding to the same areas are grouped together and present similar behaviors, the lines for squares and triangles are not overlapped, and their convergence values differ. This is different than expected, as Weyl's law is indicated to hold independent of the geometry of the domain.

However, as $\lim_{R\to\infty} \frac{N(R)}{R}$ converges, we are able to analyze its relation with A. Figure 6 presents such relationship again for squares and triangles, and for a sample of 20 areas between 1 and 100 units. We approximate $\lim_{R\to\infty} \frac{N(R)}{R}$ with R taking the value of the largest eigenvalue obtained.

As observed in Figure 6, there is indeed a linear relationship between A and $\lim_{R\to\infty} \frac{N(R)}{R}$. The red line presents the equation obtained by fitting all the data points. However, there is also a consistent bias between the points from square meshes and triangle meshes. Fitting those subsets independently yields slopes with slightly different values, which proposes the hypothesis of a dependence of the slope C with the geometry of the domain $C = C(\Omega)$. This deviates deeply from Weyl's law.

To statistically verify this, we fitted the linear relation with a new set of 100 areas from 1 to 1000, for both squares and triangles, and did a statistical test to the linear regressions to verify whether the slopes where different with statistical significance. The statistical estimator used was [12]:

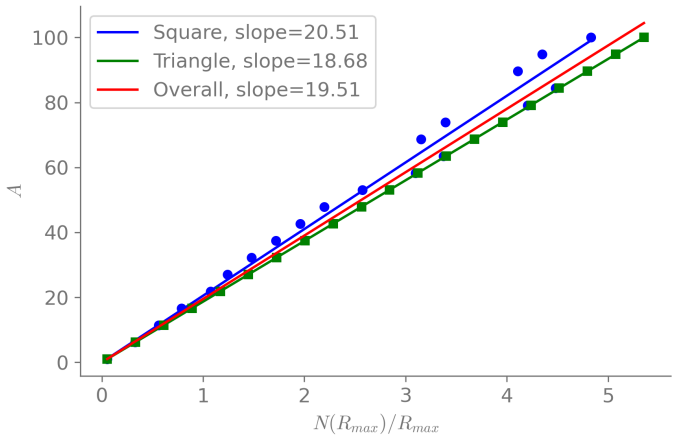

Figure 6: Linear relation between area and $\lim_{R\to\infty} \frac{N(R)}{R}$. The red line is obtained by fitting with both squares and triangles data points. Notice the slopes calculated with the different subsets differ.

$$Z = \frac{C_1 - C_2}{\sqrt{SEC_1^2 + SEC_2^2}}, \tag{11}$$

where C_1, C_2 are the slopes tested and SEC_1, SEC_2 are their standard errors according to the linear regression. Evaluating this estimator against the t-student distribution yields a significance value $p << 0.01$, which means the slopes are statistically-proven different. In other words, we conclude that, even the linear relationship given by Weyl's law holds for A and $\lim_{R\to\infty} \frac{N(R)}{R}$, the slope that relates them depends on the geometric characteristics of the domain for the wave propagation operator.

4 Conclusions

We studied the behavior of the eigenvalues of the differential operator that describes wave propagation phenomena in classical elastodynamics, for the 2D case. We set up the equations for wave propagation parting from variational principles to derive the weak form of the corresponding differential equations directly, and discretized the metric space embedding the problem, thus obtaining a finite-dimensional representation of the operator that allowed us to estimate the eigenvalues and eigenfunctions of the original differential operator as well as their overall behavior.

We applied that modeling strategy to study two scenarios among the spectral analysis of the operator. In the first one, we found that not all the domains that are isospectral with respect to the Laplacian operator keep that property with respect to the studied operator, although some of them may still do. The answer of specifically which geometric properties must the domains satisfy in order to keep the isospectral behavior must be answered by tackling this problem with a more theoretical approach, which is outside the scope of this experimental exploration.

In the second exploration, we verified the linear relation between the area of the domain and the behavior of the growth rate of the eigenvalues, based on Weyl's law for the Laplacian. However, the coefficient of that relation presents a dependence on the geometry of the domain. This is cumbersome, as it requires previous knowledge of the domain to some extent, which is expected to be unknown if one is required to calculate the are via this sort of analysis.

In order to better assess the effect of the geometry in the slope, we require to carry on the same tests on many more different geometries, or even random-generated ones in which one can estimate the are via computational methods. Furthermore, a more robust and theoretical approach in this matter is also required to give answers on the causes of the behaviors found here.

The effects of the variation of material parameters were not studied in neither of the cases, and would be a good starting point for a future work. Overall, the tools and experimental results presented here are solid enough to assist theoretical mathematicians that tackle this problem from a formal

perspective, to get clues on the behavior and properties of the mathematical structures studied and verify hypothesis and get intuitions that help their research.

A Remarks on the computational implementation

The FEM method proposed was implemented for triangular 6-node elements and quadratic form functions, with the use of Solidspy [13], in Python. As for the material parameters, a linear isotropic homogeneous material was assumed, using a unit system where the Young modulus $E = 1A.U$, density $\rho = 1A.U$, and using a typical Poisson modulus of 0.3. For the different analysis carried, several meshes had to be computed programmatically, which was done through the use of Gmsh API for Python [14]. Also, the generalized eigenmodes problem as presented was solved by means of the function *scipy.sparse.linalg.eigsh* [15]. All the code is available and completely reproducible from the open-access repository here

References

[1] J. D. Achenbach, *Wave Propagation in Elastic Solids*, en. North-Holland Publishing Company, 1973, Google-Books-ID: jQFAAQAAIAAJ, ISBN: 978-0-444-10465-6.

[2] A. D. Pierce, *Acoustics: An Introduction to Its Physical Principles and Applications*, en. Springer, Jun. 2019, Google-Books-ID: MAGfDwAAQBAJ, ISBN: 978-3-030-11214-1.

[3] M. Kac, "Can One Hear the Shape of a Drum?" en, *The American Mathematical Monthly*, vol. 73, no. 4, p. 1, Apr. 1966, ISSN: 00029890. DOI: 10.2307/2313748. [Online]. Available: https://www.jstor.org/stable/2313748?origin=crossref (visited on 03/06/2024).

[4] H. Weyl, "Nachrichten von der Gesellschaft der Wissenschaften zu Göttingen, Mathematisch-Physikalische Klasse," 1911, Context Object: ctx_ver=Z39.88-2004&rft_val_fmt=info%3Aofi%2Ffmt%3Akev%3Amtx' Physikalische%20Klasse&rft.au=&rft.pub=.

[5] R. Seeley, "A sharp asymptotic remainder estimate for the eigenvalues of the Laplacian in a domain of $R3$," *Advances in Mathematics*, vol. 29, no. 2, pp. 244–269, Feb. 1978, ISSN: 0001-8708. DOI: 10.1016/0001-8708(78)90013-0. [Online]. Available: https://www.sciencedirect.com/science/article/pii/0001870878900130 (visited on 03/06/2024).

[6] W. A. Strauss, *Partial Differential Equations: An Introduction*, en. John Wiley & Sons, Limited, Feb. 2019, Google-Books-ID: F0v3wAEACAAJ, ISBN: 978-1-119-58986-0.

[7] J. N. Reddy, *Energy Principles and Variational Methods in Applied Mechanics*, en. John Wiley & Sons, Aug. 2017, Google-Books-ID: wqUlDwAAQBAJ, ISBN: 978-1-119-08737-3.

[8] N. Guarín-Zapata, J. Gomez, A. R. Hadjesfandiari, and G. F. Dargush, "Variational principles and finite element Bloch analysis in couple stress elastodynamics," *Wave Motion*, vol. 106, p. 102 809, Nov. 2021, ISSN: 0165-2125. DOI: 10.1016/j.wavemoti.2021.102809. [Online]. Available: https://www.sciencedirect.com/science/article/pii/S0165212521001074 (visited on 12/05/2023).

[9] K.-J. Bathe, *Finite Element Procedures*, en. Prentice Hall, 1996, Google-Books-ID: buMbAAAACAAJ, ISBN: 978-0-13-301458-7.

[10] B. Ghojogh, F. Karray, and M. Crowley, *Eigenvalue and Generalized Eigenvalue Problems: Tutorial*, arXiv:1903.11240 [cs, stat], May 2023. [Online]. Available: http://arxiv.org/abs/1903.11240 (visited on 04/23/2024).

[11] P. Buser, J. Conway, P. Doyle, and K.-D. Semmler, "Some planar isospectral domains," *International Mathematics Research Notices*, vol. 1994, no. 9, pp. 391–400, Jan. 1994, ISSN: 1073-7928. DOI: 10.1155/S1073792894000437. [Online]. Available: https://doi.org/10.1155/S1073792894000437 (visited on 04/19/2024).

[12] R. Paternoster, R. Brame, P. Mazerolle, and A. Piquero, "Using the Correct Statistical Test for the Equality of Regression Coefficients," en, *Criminology*, vol. 36, no. 4, pp. 859–866, 1998, _eprint: https://onlinelibrary.wiley.com/doi/pdf/10.1111/j.1745-9125.1998.tb01268.x, ISSN: 1745-9125. DOI: 10.1111/j.1745-9125.1998.tb01268.x. [Online]. Available: https://onlinelibrary.wiley.com/doi/abs/10.1111/j.1745-9125.1998.tb01268.x (visited on 04/23/2024).

[13] N. Guarín-Zapata, *Nicoguaro/SolidsPy*, original-date: 2020-06-17T16:41:35Z, Aug. 2021. [Online]. Available: https://github.com/nicoguaro/SolidsPy (visited on 04/23/2024).

[14] C. Geuzaine and J.-F. Remacle, "Gmsh: A 3-D finite element mesh generator with built-in pre- and post-processing facilities," en, *International Journal for Numerical Methods in Engineering*, vol. 79, no. 11, pp. 1309–1331, 2009, _eprint: https://onlinelibrary.wiley.com/doi/pdf/10.1002/nme.2579, ISSN: 1097-0207. DOI: 10.1002/nme.2579. [Online]. Available: https://onlinelibrary.wiley.com/doi/abs/10.1002/nme.2579 (visited on 04/23/2024).

[15] *Scipy.sparse.linalg.eigsh — SciPy v1.13.0 Manual*. [Online]. Available: https://docs.scipy.org/doc/scipy/reference/generated/scipy.sparse.linalg.eigsh.html (visited on 04/23/2024).